CAD MODEL TO COMPUTE THE INPUT IMPEDANCE OF AN EQUILATERAL TRIANGULAR MICROSTRIP PATCH ANTENNA WITH RADOME

M. Biswas

Department of Electronics
West Bengal State University
Berunanpukuria, P.O. Malikapur, North 24 Parganas
PIN 700 126, India

A. Mandal

Department of Electronics and Communication Engineering
Future Institute of Engineering and Management
Kolkata 700 150, India

Abstract—A very simple and more efficient CAD model is proposed to demonstrate the effect on input impedance characteristics based on cavity model analysis for wide range of superstrate parameters and feed locations of an equilateral triangular microstrip patch antenna having different side lengths. The computed values are compared with different theoretical and experimental values available in open literature, showing close agreement. A Maxwell's equation solver is also used to validate our model.

1. INTRODUCTION

The triangular geometry is a narrow band structure. It can be used advantageously in designing microstrip compact array [3] with reduced coupling between adjacent elements and band pass filters [5]. Narrow impedance bandwidth may be a critical requirement for an antenna particularly for receiving a narrow band signal in the presence of noise. It can also be used on curved surfaces because of easy conformability. The triangular geometry has been investigated by many researchers [3–7, 9, 10, 13, 14, 16–19, 21, 22]. In those studies, they have not employed any dielectric superstrate in the form of radome above the patch. This radome protects the patch from the environmental hazards and

---

Corresponding author: M. Biswas (mbiswas@ieee.org).

improves the antenna performances [12, 20]. The triangular microstrip patch (TMP) with radome is the least investigated geometry. A few researchers [1, 2, 12, 15] have considered the effect of radome on the performances of TMP. Among them, [12] has shown the gain enhancement technique using a dielectric cover of a chip resistor loaded TMP, and some theoretical results of a TMP including radome have been reported in [15] using Spectral Domain Techniques (SDT). Neither any experimental result nor any design guideline is available in [12] and [15] to estimate the resonant frequency and input impedance of a TMP with radome. But [2] has reported a design guideline and experimental results for resonant frequency and input impedance of a TMP including radome effect. A very simple and efficient CAD model is reported in [1] very recently to estimate the operating frequency of a superstrate loaded TMP using cavity model analysis.

In order to calculate the input impedance of an equilateral triangular microstrip patch (ETMP) only two papers by Biswas and Guha [2] and Lee et al. [18] are available. But [18] has used rigorous mathematical steps to calculate the total quality factor (Q_T) for an ETMP without superstrate (conventional), and there is a big discrepancy between measured and theoretical values. The most recent paper [2] has reported a simple way to calculate the input impedance for conventional and superstrate loaded ETMP employing an equivalence relation between rectangular and triangular geometries to compute the total quality factor (Q_T).

In this paper, we have proposed a simpler and more efficient CAD model to estimate the effect of superstrate on input impedance characteristics of an ETMP avoiding equivalence relation and rigorous mathematical steps for calculating Q_T based on cavity model analysis.

Our computed values for wide range of superstrate parameters and feed locations of an ETMP antenna having different side lengths are compared with theoretical and experimental values, showing close agreement. The structure is also studied employing a Maxwell's equation solver [8], and those results are also used to validate the computed values determined using the present model.

2. THEORETICAL FORMULATIONS

For achieving the optimum performance the accurate calculation of input impedance of the microstrip antenna is necessary. So we have proposed a CAD model based on cavity model analysis for computing the input impedance of superstrate loaded triangular microstrip patch antenna. The superiority of this model is that this model is valid for triangular patch without superstrate (conventional). The coaxial
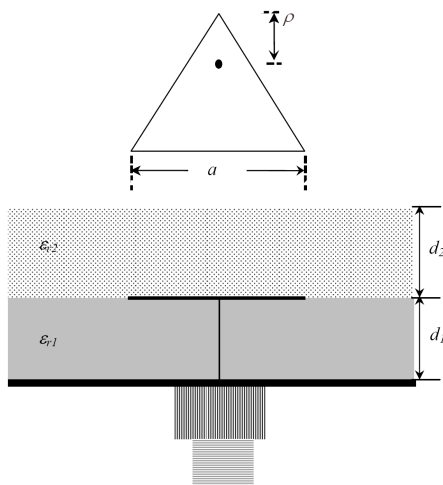
Figure 1. Probe-fed superstrate loaded equilateral triangular microstrip patch. A schematic diagram.

fed substrate-superstrate combined geometry of an ETMP antenna is shown in Fig. 1. The lower one is substrate (thickness d_1 and permittivity ε_{r1}) and upper one being superstrate (thickness d_2 and permittivity ε_{r2}).

The input impedance of a triangular microstrip patch with and without superstrate seen by the coaxial feed, located at a distance ρ from the tip of the triangle shown in Fig. 1, is given by [2] and [18]

$$Z = R + jX$$

where,

$$R = 2\pi f \mu \sum_{n=0}^{\infty} \sum_{m=n}^{\infty} \frac{4\sqrt{3}d_1\, U_{mn}k^2 P_{lmn}^2}{27a^2 Q_T} \frac{1}{(2\pi)^4 \left(f^2 - f_r^2\right)^2 \mu_0^2 \varepsilon^2 + \frac{1}{Q_T^2}k^4} \quad (1)$$

$$X = -2\pi f \mu \sum_{n=0}^{\infty} \sum_{m=n}^{\infty} \frac{4\sqrt{3}d_1 U_{mn}k^2 P_{lmn}^2}{27a^2} \frac{(2\pi)^2 \left(f^2 - f_r^2\right)\mu_0 \varepsilon}{(2\pi)^4 \left(f^2 - f_r^2\right)^2 \mu_0^2 \varepsilon^2 + \frac{1}{Q_T^2}k^4} \quad (2)$$

Here the summations indicate the number of modes.

$$U_{mn} = \begin{cases} 1, & \text{if } m = n = 0 \\ 6, & \text{if } (m=0 \text{ and } n\neq 0) \text{ or } (m\neq 0 \text{ and } n=0) \text{ or } (m=n\neq 0) \\ 12, & \text{if } m \neq n \neq 0 \end{cases} \quad (3)$$

$$P_{lmn} = \left[\cos\left(\frac{2\pi l\rho}{\sqrt{3}a}\right) j_0\left(\frac{\pi lw}{\sqrt{3}a}\right) + \cos\left(\frac{2\pi m\rho}{\sqrt{3}a}\right) j_0\left(\frac{\pi mw}{\sqrt{3}a}\right) \right.$$

$$\left. + \cos\left(\frac{2\pi n\rho}{\sqrt{3}a}\right) j_0\left(\frac{\pi nw}{\sqrt{3}a}\right) \right] \tag{4}$$

$$j_0(x) = \sin(x)/x \quad Q_T = \left(\frac{1}{Q_r} + \frac{1}{Q_d} + \frac{1}{Q_c}\right)^{-1} \quad k = k_r\sqrt{\varepsilon_{re}} \quad \varepsilon = \varepsilon_{re}\varepsilon_0 \tag{5}$$

$w = 6\,\text{mm}$ as in [2] and [18].

The quantities Q_r, Q_d, and Q_c are the quality factors due to radiation loss, dielectric loss and conductor loss respectively. Surface wave loss is neglected.

In order to calculate the total quality factor the computation of Q_r is more important because it is the key factor to determine the radiation efficiency. But the computation of Q_r is complicated for triangular geometry because of its radiation mechanism. For computing Q_r, Lee et al. [18] has employed rigorous mathematical steps, and they are not suitable due to large error between measured and theoretical values. Recently, an equivalence relation between rectangular and triangular geometry for computing Q_r has been reported by Biswas and Guha [2], which is more accurate and simpler compared to [18]. To the best of our knowledge, this is the first time we have proposed a very simple and more accurate theoretical formula without employing the equivalence relation and rigorous mathematical steps used by [2] and [18] to compute the Q_r.

So the quantity Q_r is taken empirically in this study as

$$Q_r = \frac{c\sqrt{\varepsilon_{re}}}{1.635\, f_r\, d_1} \tag{6}$$

Here, c is the velocity of light in free space, and ε_{re} is the effective dielectric constant of the substrate-superstrate combined geometry. f_r is the resonant frequency of an ETMP with superstrate.

The Quality factor due to dielectric loss (Q_d) can be computed using [11] which is simpler compared to [2] and [18] as

$$Q_d = \frac{1}{\tan\delta} \tag{7}$$

The quality factor due to conductor loss is calculated employing [2] as

$$Q_c = d_1\sqrt{\pi f_r \mu_0 \sigma} \tag{8}$$

The percent bandwidth (V.S.W.R < 2) of the antenna is calculated as

$$\frac{1}{\sqrt{2}\,Q_T}\,100\,\% \tag{9}$$

Here f_r and ε_{re} can be calculated using [1] as

$$f_r = \frac{2c}{3a_e\sqrt{\varepsilon_{re}}}(n^2 + nm + m^2)^{1/2} \tag{10}$$

$$\varepsilon_{re} = \varepsilon_{r1}v_1 + \varepsilon_{r1}(1 - v_1)^2 \times [\varepsilon_{r2}^2 v_2 v_3 + \varepsilon_{r2}\{v_2 v_4 + (v_3 + v_4)^2\}]$$
$$\times[\varepsilon_{r2}^2 v_2 v_3 v_4 + \varepsilon_{r1}(\varepsilon_{r2}v_3 + v_4)(1 - v_1 - v_4)^2 + \varepsilon_{r2}v_4\{v_2 v_4 + (v_3 + v_4)^2\}]^{-1} \tag{11}$$

The computation details of v_1, v_2, v_3 and v_4 are available in [1].

3. RESULTS AND DISCUSSIONS

Figure 2 demonstrates the variation of input resistance at resonance as a function of frequency of a superstrate loaded ETMP having side length $a = 20.3\,\text{mm}$, and feed is located at $\rho = 10.5\,\text{mm}$ from the tip of the triangle. In this plot, the thickness and dielectric constant of superstrate and substrate are chosen identical. Here we have compared our computed values with measured and computed ones as reported in [2]. From this plot it is evident that the calculated values of input impedance employing present model are close to the experiment [2] compared to the theory [2].

Table 1 shows the comparative studies of the resonant frequencies and resonant resistances for wide range of the superstrate parameters (ε_{r2} and d_2) of an ETMP. Here the computed values of present model are compared with the computed values in [2], CFDTD simulated values in [8] and SDT analysis in [15], showing close agreement.
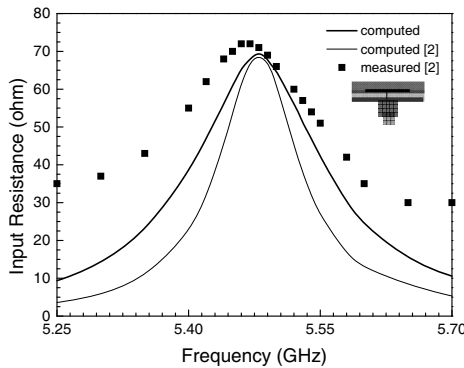
Figure 2. Measured and computed input resistance near dominat mode resonant frequency as a function of frequency of an ETMP with superstrate. $a = 20.3\,\text{mm}$, $d_1 = 1.575\,\text{mm}$, $\varepsilon_{r1} = 2.33$, $d_2 = 1.00d_1$, $\varepsilon_{r2} = 1.00\varepsilon_{r1}$, $\rho = 10.5\,\text{mm}$, $Q_T = 31.0$, $f_{rth} = 5.479\,\text{GHz}$, $f_{rmea} = 5.473\,\text{GHz}$, $\tan\delta_1 = \tan\delta_2 = 0.001$.

Table 1. Resonant frequencies and resonant resistances of an ETMP with superstrate having different thicknesses and dielectric constants: computed values compared with calculated and simulated values.

$a = 37$ mm, $d_1 = 1.59$ mm, $\varepsilon_{r1} = 2.5$, $\tan\delta_l = \tan\delta_2 = 0.0025$, $\rho = 13.5$ mm
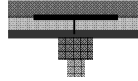
d_2/d_1	$\varepsilon_{r2}/\varepsilon_{r1}$	Resonant Frequency (GHz)				Resonant Resistance (ohm)			
		Theory [1]	Theory [2]	CFDTD [8]	SDT [15]	Theory [Present]	Theory [2]	CFDTD [8]	SDT [15]
0.50	0.6	3.177	3.14	3.19	----	435	433	435	----
	1.0	3.16	3.11	3.17	----	433	429	441	----
	1.28	3.14	3.098	3.15	----	441	425	443	----
	2.0	3.11	3.06	3.13	----	442	419	439	----
1.00	0.6	3.17	3.13	3.20	3.25	435	433	445	385
	1.0	3.14	3.095	3.15	3.17	439	426	440	400
	1.28	3.12	3.07	3.13	3.12	441	420	450	420
	2.0	3.08	3.01	3.06	----	443	410	447	----
2.00	0.6	3.16	3.125	3.16	----	434	432	445	----
	1.0	3.12	3.07	3.125	----	436	420	430	---
	1.28	3.09	3.04	3.07	---	442	413	432	----
	2.0	3.03	3.03	2.9	----	450	385	434	----
4.00	0.6	3.158	3.12	3.14	----	437	430	441	----
	1.0	3.10	3.05	3.11	----	442	419	435	---
	1.28	3.07	3.0	3.05	---	447	412	440	---
	2.0	2.995	2.91	2.85	---	456	400	450	---
0.50	0.6	3.177	3.14	3.19	---	435	433	435	----
1.00		3.17	3.13	3.20	----	435	433	445	----
2.00		3.16	3.125	3.16	----	434	432	445	-----
4.00		3.158	3.12	3.14	-----	437	430	441	----
0.50	1.0	3.16	3.11	3.17	3.21	433	429	441	420
1.00		3.14	3.095	3.15	3.16	439	426	440	410
2.00		3.12	3.07	3.125	3.09	441	420	430	370
4.00		3.10	3.05	3.11	-----	442	419	435	-----
0.50	1.28	3.14	3.098	3.15	----	439	425	443	----
1.00		3.12	3.07	3.13	----	436	420	450	----
2.00		3.09	3.04	3.07	----	442	419	432	----
4.00		3.07	3.0	3.05	----	447	412	440	----
0.50	2.0	3.11	3.06	3.13	----	442	419	439	----
1.00		3.08	3.01	3.06	----	443	410	447	----
2.00		3.03	3.03	2.9	-----	450	385	434	-----
4.00		2.995	2.91	2.85	-----	456	400	450	-----

The effect of superstrate parameters on input impedance characteristics of an ETMP is shown in Fig. 3. Here we have calculated the input impedance as a function of frequency employing present theory for different values of ε_{r2} and d_2. In these studies, we have taken $a = 50$ mm, $d_1 = 1.59$ mm, $\varepsilon_{r1} = 2.32$, and feed is located near 50 ohm point at resonance. It is evident from this plot that the resonant
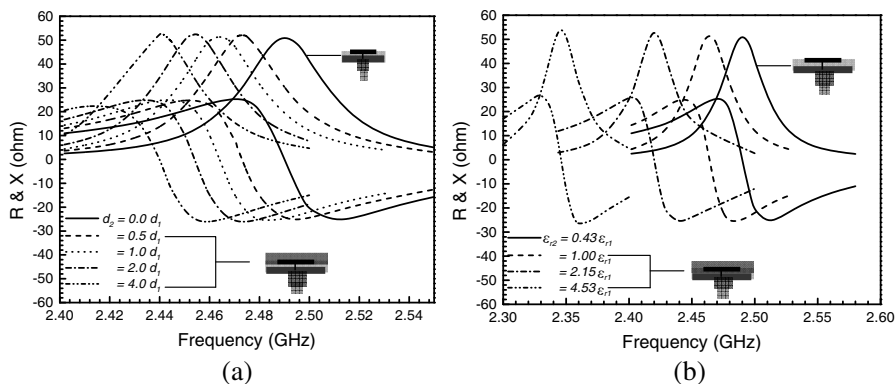
Figure 3. Computed dominant mode input impedance versus frequency of an ETMP for different values of d_2 and ε_{r2}. $a = 50\,\text{mm}$, $d_1 = 1.59\,\text{mm}$, $\varepsilon_{r1} = 2.32$, $\rho = 25.2\,\text{mm}$, $\tan\delta_1 = \tan\delta_2 = 0.0005$. (a) $\varepsilon_{r2} = 1.00\varepsilon_{r1}$ and d_2 variable. (b) $d_2 = 1.00d_1$ and ε_{r2} variable.
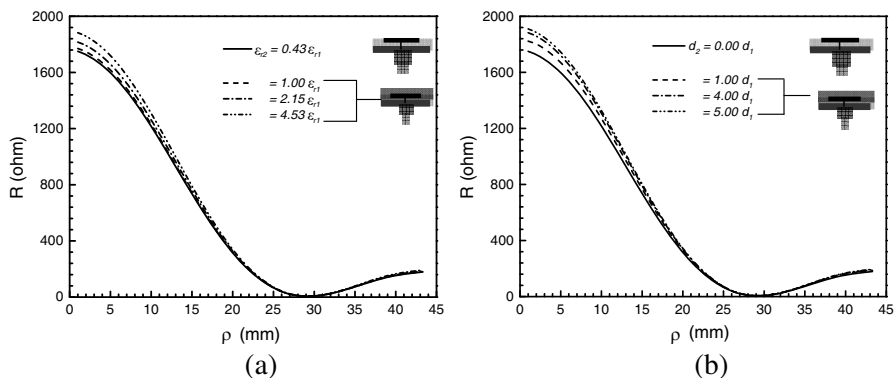
Figure 4. Computed dominant mode input resistance versus ρ of an ETMP for different values of d_2 and ε_{r2}. (a) $d_2 = 4.00d_1$ and ε_{r2} variable. (b) $\varepsilon_{r2} = 4.53\varepsilon_{r1}$ and d_2 variable. Other parameters as in Fig. 3.

frequency decreases significantly with increase in ε_{r2} as well as d_2, but the change in resonant resistance is insignificant. The percentage shifts in $f_{r,10}[\{(f_{r,10withoutsuperstrate} - f_{r,10withsuperstrate})/f_{r,10withoutsuperstrate} \cdot 100\%]$ with the variations of d_2 and ε_{r2} with respect to the patch without superstrate for $d_2 = 0.5d_1, 1.0d_1, 2.0d_1$ and $4.0d_1$ are 0.68%, 1.04%, 1.44% and 2.0% respectively and that of 1.04%, 2.8% and 5.78% for $\varepsilon_{r2} = 1.00\varepsilon_{r1}$, $2.15\varepsilon_{r1}$ and $4.53\varepsilon_{r1}$ respectively. Again from this

plot it is clear that the resonant frequency shift is more stringent in higher values of superstrate parameters. Hence it is possible to tune the antenna with superstrate.

Figure 4 depicts the variation of input resistances at resonance with feed locations (ρ) for different values of superstrate parameters. Fig. 4(a) shows these variations for $d_2 = 4.0d_1$ taking ε_{r2} as parameter and that in Fig. 4(b) for $\varepsilon_{r2} = 4.53\varepsilon_{r1}$ considering d_2 as parameter. It is evident from these plots that the change in input resistances is more significant for higher values of superstrate parameters and when the feed is located near the tip of the triangle. Again this change is insignificant when the feed points are far from the tip of the triangle.

The effect of superstrate on bandwidth is shown in Fig. 5. In this plot we have studied the variation of % bandwidth and effective dielectric constant (ε_{re}) as a function of ε_{r2} for different values of d_2. From this plot it is observed that ε_{re} increases with the increase of d_2 where as % bandwidth decreases with the increase of d_2.

That the present model is also valid for triangular patch without superstrate is visualized in Figs. 6 and 7. The variation of input resistance at resonance with feed locations (ρ) for different antenna parameters are depicted in Fig. 6. Here our computed values are compared with different measured values [2, 15, 18], showing excellent agreement. In Fig. 7, we have compared our calculated values with measured ones [15], and good agreement is revealed.
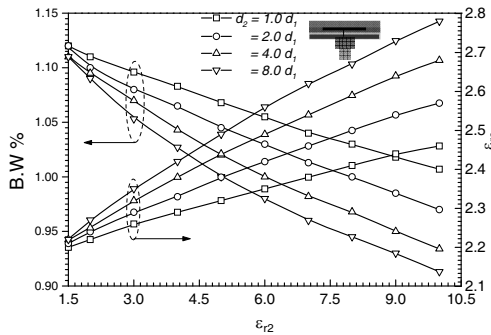

Figure 5. Theoretical variation of percent bandwidth and ε_{re} as a function of ε_{r2} for different values of d_2 of an ETMP. Parameters as in Fig. 3.
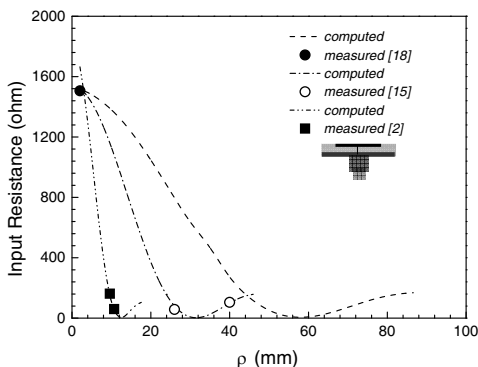
Figure 6. Measured and computed dominant mode input resistance versus ρ of an ETMP without superstrate. $\mathbf{-\,-\,-}$ and $\bullet$: $a = 100\,\text{mm}$, $d_1 = 1.59\,\text{mm}$, $\varepsilon_{r1} = 2.32$, $\tan\delta_1 = 0.0005$, $f_{r,th} = 1.282\,\text{GHz}$. $\mathbf{-\,.\,.}$ and $\bigcirc$: $a = 54\,\text{mm}$, $d_1 = 1.59\,\text{mm}$, $\varepsilon_{r1} = 2.5$, $\tan\delta_1 = 0.0025$, $f_{r,th} = 2.24\,\text{GHz}$. $\mathbf{-\,.\,.}$ and $\blacksquare$: $a = 20.3\,\text{mm}$, $d_1 = 1.575\,\text{mm}$, $\varepsilon_{r1} = 2.33$, $\tan\delta_1 = 0.001$, $f_{r,th} = 5.61\,\text{GHz}$.
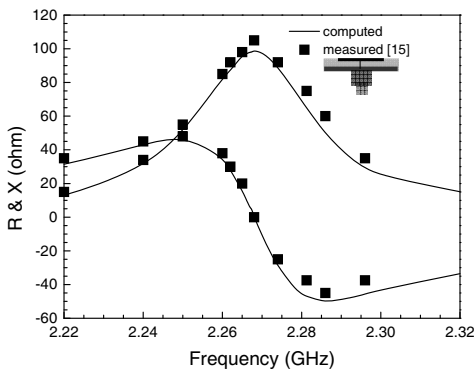
Figure 7. Measured and computed dominant mode input impedance as a function of frequency for coaxial fed ETMP with out superstrate. $a = 54\,\text{mm}$, $d_1 = 1.59\,\text{mm}$, $d_2 = 0\,\text{mm}$, $\varepsilon_{r1} = 2.5$, $\rho = 40\,\text{mm}$, $\tan\delta_1 = 0.0025$.

4. CONCLUSIONS

The effect of superstrate on input impedance characteristics is theoretically investigated. The computed values for wide range of variation of superstrate parameters and feed locations of an ETMP having different side lengths are compared with theoretical and

experimental values, which reveals close agreement. The superiority of this model is that it is also valid for conventional triangular geometry without superstrate. This formula is very important for practical design and implementation.

REFERENCES

1. Biswas, M. and A. Mandal, "The effect of radome on resonance characteristics of an equilateral triangular microstrip patch antenna," *Journal of Microwaves, Optoelectronics and Electromagnetic Applications*, 2010.

2. Biswas, M. and D. Guha, "Input impedance and resonance characteristic of superstrate loaded triangular microstrip patch," *IET Microw. Antennas Propagat.*, Vol. 3, 92–98, Feb. 2009.

3. Sumantyo, J. T. S., K. Ito, and M. Takahashi, "Dual-band circularly polarized equilateral triangular-patch array antenna for mobile satellite communications," *IEEE Trans. Antennas Propagat.*, Vol. 53, No. 11, 3477–3485, Nov. 2005.

4. Nasimuddin, K. E. and A. K. Verma, "Resonant frequency of an equilateral triangular microstrip antenna," *Microwav. Opt. Tech. Lett.*, Vol. 47, No. 5, 485–489, Dec. 2005.

5. Hong, J.-S. and M. J. Lancaster, "Theory and experiment of dual-mode microstrip triangular patch resonators and filters," *IEEE Trans. Microwave Theory Tech.*, Vol. 52, No. 4, 1237–1243, Apr. 2004.

6. Guha, D. and J. Y. Siddiqui, "Resonant frequency of equilateral triangular microstrip patch antenna with and without air gaps," *IEEE Trans. Antennas Propagat.*, Vol. 52, No. 8, 2174–2177, Aug. 2004.

7. Nasimuddin, S. and A. K. Verma, "Fast and accurate model for analysis of equilateral triangular microstrip patch," *Journal of Microwaves and Optoelectronics*, Vol. 3, 90–110, 2004.

8. Yu, W. and R. Mittra, *Conformal Finite Difference Time Domain Maxwell's Equation Solver, Software and User's Guide*, Artech House, 2004.

9. Lu, J.-H. and K.-L. Wong, "Single-feed circularly polarized equilateral triangular microstrip antenna with a tuning stub," *IEEE Trans. Antennas Propagat.*, Vol. 48, 1869–1872, 2000.

10. Gurel, C. S. and E. Yazgan, "New computation of the resonant frequency of a tunable equilateral triangular microstrip patch," *IEEE Trans. Microwave Theory Tech.*, Vol. 48, 334–338, 2000.

11. Garg, R., P. Bhartia, I. Bahl, and A. Ittipiboon, *Microstrip Antenna Design Handbook*, Artech House, 2000.

12. Hong, C.-S., "Gain-enhanced broadband microstrip antenna," *Proc. Natl. Sci. Counc. ROC(A)*, Vol. 23, No. 5, 609–611, 1999.

13. Karaboğa, D., K. Güney, N. Karaboğa, and A. Kaplan, "Simple and accurate effective side length expression obtained by using a modified genetic algorithm for the resonant frequency of an equilateral triangular microstrip antenna," *Int. J. Electron.*, Vol. 83, 99–108, Jan. 1997.

14. Mirshekar Syahkal, D. and H. R. Hassani, "Characteristics of stacked rectangular and triangular patch antennas for dual band applications," *8th IEE International Conference on Antennas and Propagat.*, 728–731, 1993.

15. Hassani, H. R. and D. Mirshekar Syahkal, "Analysis of triangular patch antennas including radome effects" *IEE Proceedings H*, Vol. 139, No. 3, 251–256, Jun. 1992.

16. Chen, W., K. F. Lee, and J. S. Dahele, "Theoretical and experimental studies of the resonant frequencies of equilateral triangular microstrip antenna," *IEEE Trans. Antennas Propagat.*, Vol. 40, 1253–1256, Oct. 1992.

17. Gang, X., "On the resonant frequencies of microstrip antennas," *IEEE Trans. Antennas Propagat.*, Vol. 37, 245–247, 1989.

18. Lee, K. F., K. M. Luk, and J. S. Dahele, "Characteristics of the equilateral triangular patch antenna," *IEEE Trans. Antennas Propagat.*, Vol. 36, No. 11, 1510–1518, Nov. 1988.

19. Dahele, J. S. and K. F. Lee, "On the resonant frequencies of the triangular patch antenna," *IEEE Trans. Antennas Propagat.*, Vol. 35, 100–101, 1987.

20. Alexopoulos, N. G. and D. R. Jackson, "Fundamental superstrate (cover) effects on printed circuit antennas," *IEEE Trans. Antennas Propagat.*, Vol. 32, 807–816, Aug. 1984.

21. Keuster, E. F. and D. C. Chang, "A geometrical theory for the resonant frequencies and Q factors of some triangular microstrip patch antenna," *IEEE Trans. Antennas Propagat.*, Vol. 31, 27–34, 1983.

22. Helszajn, J. and D. S. James, "Planar triangular resonators with magnetic walls," *IEEE Trans. Microwave Theory Tech.*, Vol. 26, 95–100, Feb. 1978.